KES Transactions on Sustainable Design and Manufacturing I
Sustainable Design and Manufacturing 2014 : pp.691-702 : Paper sdm14-094

Influences of a High Frequency Induction Current on the Uniformity of the Magnetic Field in an Electromagnetic Casting Mould

Lintao Zhang, Ian Cameron and Johann Sienz

Advanced Sustainable Manufacturing Technologies (ASTUTE), College of Engineering, Swansea University, Singleton Park, Swansea SA2 8PP, UK
L.Zhang@swansea.ac.uk

Abstract An analysis of the influences of a high frequency (30 kHz) alternating current on the uniformity of the magnetic field (**B**) in an electromagnetic casting (EMC) mould is investigated by means of parametric numerical simulations where the induction current (J_s) varies in the range of [1 to 10000 A]. The results show that values of the magnetic flux density along the casting direction (B_z) near the square mould corners are small, compared to those at the other locations where J_s < 10000 A, and that the magnitude of B_z increases with an increased induction current (J_s). Furthermore, it is shown that, for the EMC mould structure investigated in this paper, the increase of J_s worsen the uniformity of the magnetic, especially for the regions near molten steel level. Moreover, the effective acting region (R_{bz}) for the critical magnetic field (B_z^c) is first introduced in this paper, which opens an interesting topic for future research.

1. Introduction and principles of electromagnetic casting technique

This paper focuses on investigations into the influences of the induction current (J_s) on the uniformities of the magnetic field (**B**) in a square electromagnetic casting (EMC) mould. The approach consists of a variety of numerical simulations to reveal the distributions of the magnetic flux density along the casting direction (B_z), which are obtained when the value of J_s is varied.

The interest in the EMC technique, which was first applied to the aluminum casting process, stems from dramatic improvement of the surface quality of the strands[1]. The application of the EMC technique to the steel casting process has been developed in some steel casting companies[2,3]. The basic principles of EMC technique are shown in Figure 1(a). The EMC mould is surrounded by an induction coil, which is used as a carrier for the induction current (alternating current). The magnetic field (**B**) is generated in the space and the induced current (J_i) is also generated in the molten steel. With the interactions of **B** and J_i, the *Lorentz force* (**F**) acting towards the centre of the mould. The movements of the molten steel caused by the Lorentz force can improve the lubricating conditions between the strands and the mould, which result in allowing a higher casting speed together resulting in an improved production rate. Another main advantage of the EMC technique is that it can improve the surface quality of the strands so that the

strands are smooth enough to be rolled without requiring the scalping process. For round billets, the surface quality is improved significantly[4], as shown in Figure 1(b). Similarly, for square billets, the depth of the oscillation marks decreases from approximately 0.6 to 0.15 mm[5].

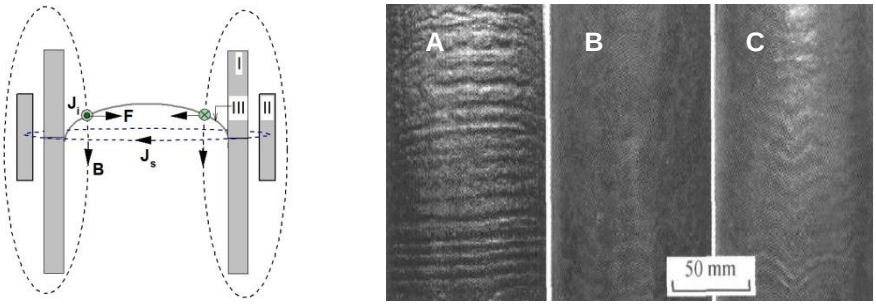

(a) (b)

Figure 1: (a): Principles of the EMC technique. *Left*: conventional continuous casting. Right: EMC. I: mold; II: induction coil and III: molten steel level. The magnetic field **B** generated by the alternating current ($\mathbf{J_s}$) in the induction coils. The *Lorentz force* is generated by the interactions between the induced current ($\mathbf{J_i}$) and **B** in the liquid metal and in the mould, and acts towards the centre of the mould. (b): The improvement of the surface quality of the round billets. A, B and C present the surface features when the input power is 0, 50.6 and 60 kW, respectively. The oscillation marks on the surface of 0.22wt% C steel are not present for input powers greater than approximately 50.6 kW.

Previous research into the EMC technique is widely reported in the literature, not only involving numerical simulations[6], but also industrial experiments[7]. The previous work has predominantly focused on the selection of frequency[8,9] of J_s, the ways to apply magnetic fields[10-12] and the influences of the mould structures on the magnetic field distributions, meniscus behavior and the surface qualities of the strands. However, from a practical point of view, the choice of the induction current (or input power) is the key problem of the industrial application of the EMC process due to economic reasons. Thus, to obtain a relatively uniform magnetic field with a wider effective range of magnetic field by using the optimum induction current for a given EMC mould structure is the dominating topic for the application of the EMC technique to commercial production. The research presented in this paper aims to determine the required input power to achieve the required magnetic field for a given mould. The approach used consists of generating the magnetic field by injecting a high frequency alternating current in the induction coil and analyzing the relationships between the current density and the uniformity of the magnetic field in the EMC mould.

The layout of this paper is as follows. The problem geometry and the numerical analysis setup are discussed in section 2. In section 3, after a short overview of B_z along casting direction in the mould, the influences the molten steel simulator together with the flange on the mould top are discussed. In section 4, the influence of J_s on the uniformity of B_z near molten steel level are presented. The effective acting region (R_{bz}) for the critical magnetic field (B_z^c) is introduced in section 5. The main conclusions are given in section 6.

2. Problem geometry and numerical analysis setup

The geometry considered in this investigation is a square mould with the inner size of 100×100 mm, which consists of 12 slits, 8 large segments (LS) and 4 corner segments (CS), as shown in Figure 2.

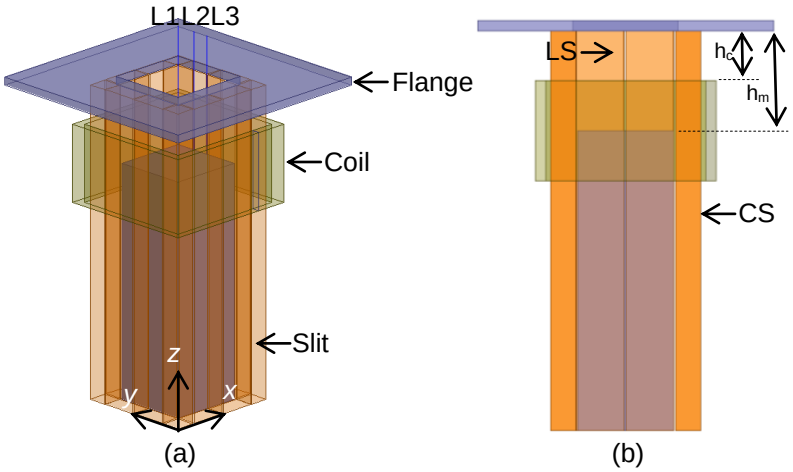

Figure 2: Three-dimensional systems for conductors and the coordinate system in the computing domain: (a) 3D view and (b) side view. The origin point is located at the bottom mould corner and the flange is placed on the top of the mould. h_c is defined as the distance between the top of the induction coil and the top of the mould. h_m is defined as the distance from the molten steel level to the top of the mould. In this research, h_c =50 mm and h_m =100 mm.

Unlike the geometries investigated in previous research, the sizes of the segments are not equal in this investigation. There are two main reasons for this choice: firstly, from a practical point of view, simple structures with a small number of mould segments are desirable in the applications of EMC technique in a realistic system. Secondly, as previously stated, the main objective for this paper is to investigate the influence of the induction current on the uniformity of the magnetic field in the mould, for which unequal sized segments provide increased sensitivity. In Figure 2, the origin is shown at the bottom of the mould. The flange, induction

coil and coordinate system are also shown in the figure. The distance between the top of the induction coil and the top of the mould (h_c) is 50 mm and the distance between the top of the molten steel and the top the mould (h_m) is 100 mm throughout the investigations reported in this paper. The detailed parameters of the EMC mould used in the numerical simulation in this investigation are shown in Table 1.

Table1. Parameters of the EMC mould for the numerical simulation.

Items	Values
Inner size of EMC mould (mm)	100×100
Height of mould (mm)	400
Height of induction coil (mm)	100
Height of liquid metal (mm)	300
Number of slits (-)	12
Height of silts (mm)	400
Width of slits (mm)	0.5
Number of corner segments (-)	4
Size of corner segment (mm)	25×25
Number of large segments (-)	8
Size of large segment (-)	49.25×26
Frequency of alternating current (kHz)	30

In the whole computing domain, the Maxwell equations can be expressed as:

$$\nabla \times \mathbf{B} = \mu_0 \mathbf{J}, \tag{1}$$

$$\nabla \times \mathbf{E} = -\frac{\partial \mathbf{B}}{\partial t}, \tag{2}$$

$$\nabla \cdot \mathbf{B} = 0, \tag{3}$$

where **J**, **E**, and μ_0 are current density, electric field and the vacuum permeability, respectively. Furthermore, $\mathbf{A}$ and ϕ are introduced as follows:

$$\mathbf{B} = \nabla \times \mathbf{A}, \tag{4}$$

$$\mathbf{E} = -\frac{\partial \mathbf{A}}{\partial t} - \nabla\phi. \tag{5}$$

This gives:

$$\nabla \times \frac{1}{\mu_0}\nabla \times \mathbf{A} - \nabla\left(\frac{1}{\mu_0}\nabla \cdot \mathbf{A}\right) + i2\pi f\sigma\mathbf{A} + \sigma\nabla\phi - \mathbf{J} = 0, \tag{7}$$

$$\nabla \cdot (-i2\pi f\sigma\mathbf{A} - \sigma\nabla\phi) = 0. \tag{8}$$

All the simulations in this paper were carried out using Ansoft Maxwell v15.0 electromagnetic field simulation software. In order to get accurate results, the meshes used were carefully generated. The skin depths for the mould (electrical conductivity $\sigma=5.96\times10^{7}$ S/m, permeability $\mu=1.26\times10^{-6}$ H/m) and molten steel simulator (electrical conductivity $\sigma=1.0\times10^{7}$ S/m, permeability $\mu=8.75\times10^{-4}$ H/m) are 0.38 mm and 2.77 mm for a 30 kHz frequency. 5 elements are controlled within the skin length. The total number of elements in the mesh for all the conductor objects is 1640763, with the mesh having increased refinement near the edges of the components. The eddy current effects of the mould and the molten steel simulator have also been taken into account. The induction current is applied to the cross-section of the induction coil as the excitation. The details of the relationship between the total energy errors and number of iterations of the numerical simulations are shown in Figure 3. In order to minimise CPU time and have reasonably accurate simulation results, all simulations were performed with 10 iterations.

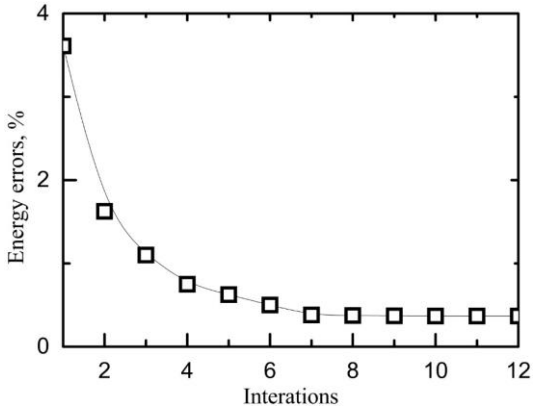

Figure 3: The relationship between the energy errors and the number of iterations of the numerical simulations, for J_s =1000 A.

3. Overview of B_z along casting direction (z) in the mould

In this section, the distribution of B_z along the z axis is presented for different values of J_s, in the range of [1 to 10000 A]. The influences of the flange, which is positioned at the top of the mould in a realistic system, and the load which is the simulation of the molten steel in the EMC mould, on the distribution of B_z are also discussed. Due to the symmetry of the square EMC mould, three lines (L1, L2 and L3) on the inner surface of a single face of the inside of the mould in the casting direction (z) were selected along which to analyse the magnetic field in the mould. L1, L2 and L3 are shown in Figure 2(a), and are located near the corner of the

square EMC mould, in the middle of a large segment and on the slit between two large segments, respectively.

The distribution of the magnetic induction vector **B** at the region near the induction coil is presented in figure 4. A magnetic field in the direction of $-z$ is shown in the region near the liquid metal, as shown in the figure.

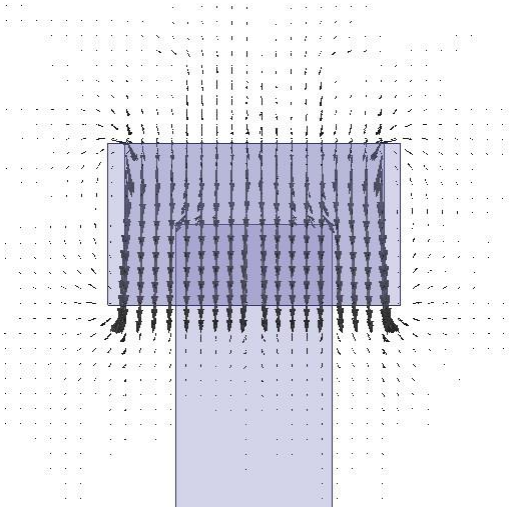

Figure 4: Distribution of magnetic induction vector **B** at the region near induction coil.

Figure 5 shows the variations of B_z along the casting direction at L1, L2 and L3 for J_s = 1000 A. Three different conditions were taken into account: with load and without flange (Condition 1: green markers and lines), with load and with flange (Condition 2: blue markers and lines) and without load and without flange (Condition 3: black markers and lines). The relative positions between coil, mould, flange and load are also shown in the figure. Firstly, for Condition 1, two relatively high values of B_z are shown along the casting direction. The first one is located near the top of the mould (z = 400 mm) and the maximum value is located just below the molten steel level (z = 350 mm). Similar results are obtained along L1, L2 and L3. The first relatively high value is explained by the part of the magnetic field that comes into the mould through the open top of the mould. Obviously, it is more important to discuss the details of the second peak value of B_z, which directly influences the initial solidification process of the strands. This maximum value of B_z is simply explained by the reflection of the magnetic field by the simulation of the molten steel. The influence of the molten steel causes the compression of the magnetic field, which permeates into the mould through the slits, to the inner surface of the mould. The peak value occurs just below the molten steel level. In

the region between the mould top and the metal level (400 < z < 350), it is shown that values of B_z near the corner region are larger than those near the middle of LS and the slit. The main reason for this is due to the two slits at the mould corner, these cause the magnetic fields to compress each other along L1. However, it is shown that the magnitude of maximum values of B_z along L2 (0.0114 T at z = 292 mm) and L3 (0.0115 T at z = 292 mm) are similar, which are 9.5% larger than those along L1 (0.0105 T at z = 292 mm). This is because the magnetic field in the region of z < 350 mm at the corner (along L1) is influenced not only by the magnetic field which permeates from the slits, but also by the induced magnetic field ($\mathbf{B}_i$, which has an opposite polarity to **B**) which is generated by the eddy current in the load. The induced magnetic field at the corner region of the molten steel is higher than at the other regions of the molten steel. This causes the decrease of the total magnetic field compared to the other locations in the mould at the same height (z). This phenomenon indicates that for designing the EMC square mould: in order to increase B_z at corner regions, it is necessary to widen the slits to some extent. In the bottom part of the mould, the B_z values do not change significantly at different locations, i.e. at L1, L2 and L3.

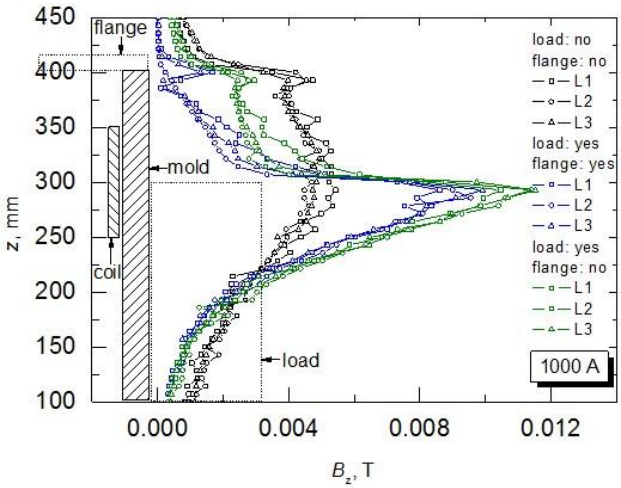

Figure 5: Comparisons of B_z along z for conditions for J_s = 1000 A. Condition 1: with load in the mould and without flange on top of the mould (in green). Condition 2 with load in the mould and without flange on the top of the mould (in blue). Condition 3 without load in the mould and without flange on the top of the mould. *Double peaks* of B_z are shown along the casting direction for the three different conditions.

Secondly, for Condition 2, the results show that the influences of the flange are not significant, especially for the initial solidification regions of the molten steel, as seen in Figure 5. This indicates that the magnetic field near that region is mainly formed by the magnetic field which permeates through the mould slits. However,

the flange can stop the magnetic flux lines which permeate into the mould through the top, which is proven by the fact that the values of B_z are lower for the Condition 2 results compared to the Condition 1 results (green in figure).

Finally, for Condition 3 the simulation also shows the influence of the molten steel. The Condition 3 results have greatly reduced peak values of Bz compared with the results from Condition 1 and Condition 2. This is simply due to the fact that the molten steel reflects the magnetic flux lines and compresses them to the inner surface of the mould, as previously discussed. This supports the fact that the effect of the molten steel must be taken into account, and will ensure accurate results for both numerical simulations and experiments.

Figure 6 shows the variations of B_z along *z,* for different values of J_s for Condition 1. It is shown that magnetic flux density increases as the induction current is increased, especially for the maximum values, which appear at the region just below the molten steel level. This is simply due to the fact that as the induction current increases, the *Lorentz force* increases in the mould and the air gap between the inner surface of the mould and the molten steel becomes wider.

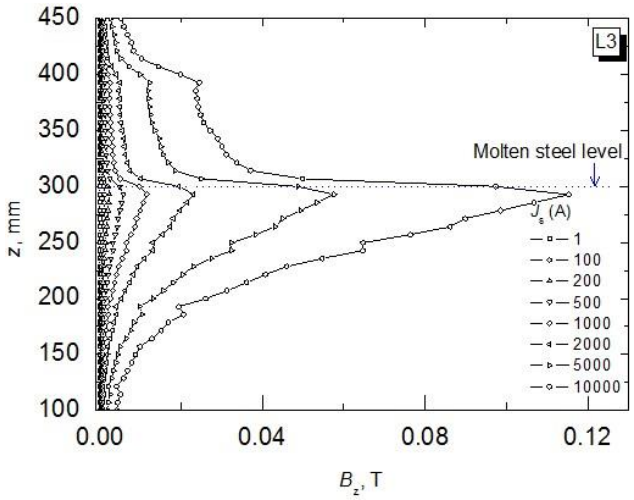

Figure 6: The variations of B_z along the casting direction (L3), for different values of J_s. The magnitude of B_z increases with increasing values of J_s, especially for the maximum values, which appear near the regions of the molten steel level.

This wider gap allows an increased application of mould flux, improving the lubrication conditions. High surface quality billets will be manufactured under these conditions. However, as a result of increasing the induction current (or input power), the fluctuations in the meniscus become more pronounced, and these fluctuations can destroy the initial solidification shell, which can directly cause more defects on the surface of the strands. Obviously a greater number of defects are contrary to

the initial aim of the electromagnetic continuous casting technique. This means that the optimum induction current should be selected to get the optimum surface finish for the minimum induction current or input power, and therefore minimise the power requirements. This is one of the most important topics for the application of the electromagnetic continuous casting technique.

4. Influence of J_s on the uniformity of B_z near molten metal level

This section first focuses on the regions where the maximum values of B_z appear and the relationships between the peak value and the induction current are discussed, as shown in Figure 7.

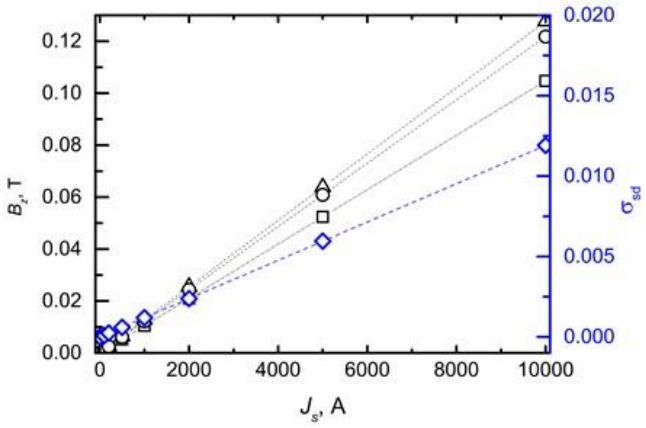

Figure 7: Comparison of B_{zmax} for different values of J_s and the uniformity of the magnetic field at z=300 mm.

For small values of induction current, such as J_s =1A, this process is effectively a quasi-traditional continuous casting (CC) process, and the amplitudes of B_z are in the order of 10^{-5}. Under this condition, the values of B_z are very uniform since the effect of the induced current is negligible. As the value of J_s increases, the non-uniform features become evident. For the mould investigated in this paper, it is found that, B_z along L2 and L3 increases much more sharply than along L1. This phenomenon is more obvious at high values of J_s. The uniformity of the magnetic field is presented by the standard deviation (σ_{sd}) of B_z at z=300 mm (in Figure 6). The results show that, for the geometry studied, the increase of J_s worsen the uniformity of the magnetic field for conditions where J_s < 10000 A. One of the effective methods to improve the uniformity of B_z is by the careful design of the corner slits, which can increase the magnetic field, as discussed in the previous sections.

5. Influence of J_S on the effective acting region (R_{Bz}) of the critical magnetic field (B_z^c)

In this section, the effective acting region R_{Bz} of the critical magnetic field B_z^c is first introduced. R_{Bz} is defined as the region in the casting direction for a given critical magnetic induction, where the magnetic induction has higher values than the critical magnetic induction and it is defined with the aim of capturing the effective acting range for a critical (or effective) magnetic field, which can support a sufficiently wide effective region for the EMC. This parameter is helpful for the selection of induction current and the locations of molten steel levels.

Figure 8 shows the relationships between R_{Bz} and B_z^c, for different values of J_S. It is found that as J_S increases, R_{Bz} increases, which is also true for different values of B_z^c. This indicates that for higher values of induction current, the molten steel level can be designed to be at an increased range of positions compared with lower values of the induction current. It is intended to further investigate the effect on the range of satisfactory locations for the height of the molten steel, the locations of the induction coils, and their scaling laws and the results will be published in future papers.

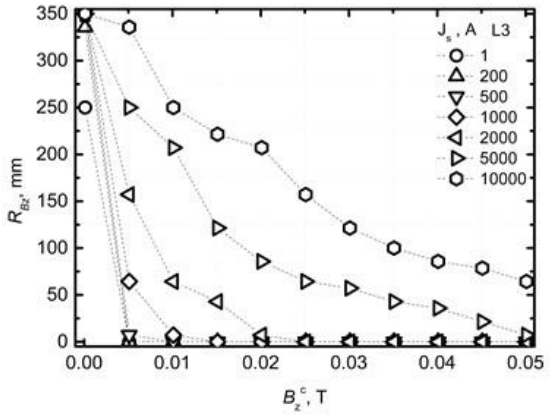

Figure 8: The variations of R_{Bz} with B_z^c, for different values of J_S. For a given critical magnetic field, the effective acting region increases with increasing induction current.

6. Conclusions

A detailed analysis of magnetic flux density distributions in a square EMC mould along with the influence of the flange cover and the molten steel were investigated by varying the high frequency (30 kHz) induction alternating current. The results which were obtained from the numerical simulations have answered the question raised in the introduction:

- for the EMC mould investigated, the magnetic field near the corner region is small compared to those at the middle of the large segment and at the slit between two large segments when J_s < 10000 A, at a frequency of 30 kHz.
- the increase of induction current can increase the magnitude of the magnetic field and worsen the uniformity of the magnetic field in the mold, especially for the regions near the molten steel level.
- in order to obtain a relatively uniform magnetic field in the square EMC mould, the corner regions should be carefully designed for actual systems.

Furthermore, the effective acting region for the critical magnetic field was first introduced. This will form a topic of future research in this field.

The authors would like to acknowledge the support of the Advanced Sustainable Manufacturing Technologies (ASTUTE) project, which is part funded from the EU's European Regional Development Fund through the Welsh European Funding Office, in enabling the research upon which this paper is based. Further information on ASTUTE can be found at www.astutewales.com.

References

[1] Vives, C.: Electromagnetic Refining of Aluminum Alloy by the CREM Process: Part I. Working Principle and Metallurgical and Results. Metallurgical Transactions B. 20B, 623-629 (1989)
[2] Mstasumiya, T.: Recent Topics of Research and Development in Continuous Casting. ISIJ International. 46,12, 1800-1804 (2006)
[3] Yasuda, H., Toh, T., and Morita, K.: Recent Progress of EPM in Steelmaking, Casting, and Solidification Processing. ISIJ International. 47,4, 619-626 (2007)
[4] Deng, A., Xu, X., Wang, E., Zhang, L., Zhang, X. and He, J: Experimental Research on Round Steel Billet Electromagnetic Soft-contact Continuous Casting Process. Iron and Steel. 44,4, 33-37 (2009)
[5] Park, J., Jeong, H., Kim, H. and Kim, J.: Laboratory Scale Continuous Casing of Steel Billet with High Frequency Magnetic Field. ISIJ International. 42,4, 385-391 (2002)
[6] Besson, O., Bourgeois, J., Chevaller, P.A., Rappaz, J., and Touzani, R.: Numerical Modeling of Electromagnetic Casting Process. Journal of Computational Physics. 92, 482-507 (1991).
[7] Park, J., Kim, H., Jeong, H., Kim, G., Cho, M.J., Yoon, M., Kim, K.R. and Choi, J. Continuous Casing of Steel Billet with High Frequency Electromagnetic Field. ISIJ International. 46,6, 813-819 (2003)

[8] Toh, T., Takeuchi, E., Hojo, M., Kawai, H. and Matsumura, S.: Electromagnetic Control of Initial Solidification in Continuous Casting of Steel by Low Frequency Alternating Magnetic Field. ISIJ International. 37,11, 1112-1119 (1997)

[9] Nakata, H., Inoue, T., Ayata, K., Murakami, T., and Kominami, T.: Improvement of Billet Surface Quality by Ultra-high-frequency Electromagnetic Casing. ISIJ International. 42,3, 264-272 (2002)

[10] Li, T., Sassa, K. and Asai, S.: Surface Quality Improvement of Continuous Casing Metals by Imposing Intermittent High Frequency Magnetic Field and Synchronizing the Field Mould Oscillation. ISIJ International. 36,4, 410-416 (1995)

[11] Lei, Z., Ren, Z., Deng, K., Li, W. and Wang, H.: Experiment Study on Mould Oscillation-less Continuous Casing Process under High Frequency Amplitude-modulated Magnetic Field. ISIJ International. 44,11, 1842-1846 (2004)

[12] Li, T., Li, X., Zhang, Z. and Jin, J.: Effect of multi-electromagnetic field on meniscus shape and quality of continuous cast metals. Ironmaking and steelmaking, 31,1, 57-60 (2006)